Verduzco-Ramírez, Arturo; Manzanilla-Dávila, Silvia Graciela; Morales-Guillén, María
Eugenia; García-Ramos, Juan Carlos; Toledano-Magaña, Yanis; Marin-Becerra,
Armando; Flores-Álamo, Marcos; Ortiz-Frade, Luis Antonio; Olguín-Contreras, Luis
Fernando; Ruiz-Azuara, Lena
Essential Metal-based drugs: Correlation between Redox Potential and Biological Activity
of M2+ with a N2O2 Ligand

Article

Essential Metal-based drugs: Correlation between Redox Potential and Biological Activity of M^{2+} with a N$_2$O$_2$ Ligand

Arturo Verduzco-Ramírez,[1] Silvia Graciela Manzanilla-Dávila,[1] María Eugenia Morales-Guillén,[2] Juan Carlos García-Ramos,[1‡] Yanis Toledano-Magaña,[1§] Armando Marin-Becerra,[1] Marcos Flores-Álamo,[1] Luis Antonio Ortiz-Frade,[3] Luis Fernando Olguín-Contreras[2] and Lena Ruiz-Azuara[1*]

[1] Departamento de Química Inorgánica y Nuclear, Facultad de Química, Universidad Nacional Autónoma de México, Avenida Universidad 3000, 04510 Mexico City, Mexico. E-mail: lenar701@gmail.com; Fax: (+) (5255)56223529

[2] Departamento Fisicoquímica, Facultad de Química, Universidad Nacional Autónoma de México, Avenida Universidad 3000, 04510 México City, Mexico.

[3] Electrochemistry Department, Centro de Investigación y Desarrollo Tecnológico en Electroquímica S.C. Parque Tecnológico Querétaro, Sanfandila, Pedro de Escobedo, C.P. 76703 Querétaro, México

[‡] Currently as postdoctoral fellow at Instituto de Química, UNAM.

[§] Currently at Centro de Nanociencia y Nanotecnología, UNAM.

[*] Corresponding author, Lena Ruiz-Azuara. E-mail: lenar701@gmail.com; Fax: (+) (5255)56223529

This paper is dedicated to the memory of Roberto Sanchez Delgado, an outstanding Latin American scientist and very good friend.

Abstract. One of the major public health problems worldwide is cancer followed by a significant number of deaths due to the resistance developed by bacteria or protozoan to the currently employed treatments. This generates an immediate need to develop drugs to treat these afflictions (illnesses, diseases). It has recently been identified that tumor cell, bacteria or protozoa are quite sensitive to oxidative stress induced by the same drugs. Due to this, it is important to develop new drugs to attend them, in this case, by using metals to increase the concentration of oxidative species. In the present work, the ligand 2,9-diformyl-4,7-diphenyl-1,10-phenanthroline and its corresponding coordination compounds with essential metals such as iron(II), cobalt(II), nickel(II), copper(II) and zinc(II) were synthesized. The electrochemical study shows that these compounds present three redox processes, all of them associated to the ligand. The compounds have shown inhibitory activity *in vitro* against human neuroblastoma CHP-212 cells, *Escherichia coli* and trophozoites of *Entamoeba histolytica* HM1:IMSS. It has been found that the inhibitory activity of the compounds studied is related to the first reduction process of the ligand. The correlation between the inhibitory activity and the red ox potential was linear. The inhibitory activity in CHP-212 increased with the increase of the compounds' redox potential values, in contrast with the behavior observed in *Escherichia coli*, where the compounds with lowest redox potential values have had significantly higher inhibitory activity. Many of these coordination compounds have shown a higher inhibitory activity than those typically used in the treatment of cancer (cisplatin). The next step is to prove these compounds *in vitro* against healthy cells in order to verify its selectivity or cytotoxicity in these systems.
Keywords: 2,9-biformyl-4,7-biphenyl-1,10-phenanthroline; reduction; oxidation; inhibitory; IC$_{50}$

Resumen. En recientes años, muchas bacterias han desarrollado resistencia ante las medicinas comúnmente utilizadas en el tratamiento. De igual forma una de las enfermedades que ha causado muchas muertes es el cáncer. Se ha demostrado que un punto en común para ambos sistemas es su susceptibilidad al estrés oxidante. Por esta razón es importante desarrollar nuevos medicamentos para el tratamiento utilizando metales esenciales generadores de estrés oxidante. En este trabajo se sintetizó y caracterizó el ligante 2,9-diformil-4,7-difenil-1,10-fenantrolina con sus correspondientes compuestos de coordinación con metales esenciales como hierro(II), cobalto(II), níquel(II), cobre(II) y zinc(II). Estos compuestos presentaron tres procesos redox asociados al ligante. Los compuestos presentaron actividad biológica *in vitro* en células CHP-212, *Escherichia coli y* trofozoitos de *Entamoeba histolytica* HM1:IMSS. Se encontró que la actividad biológica de estos compuestos está relacionada con el primer proceso redox del ligante. Mientras mayor fue el potencial de reducción en los compuestos, mayor actividad inhibitoria en las células CHP-212 y los compuestos con menores potenciales mostraron mayor actividad biológica en *Escherichia coli*. Muchos de estos compuestos presentaron una mayor actividad inhibitoria que aquellos comúnmente utilizados en el tratamiento del cáncer (cisplatino). El siguiente paso es evaluar estos compuestos *in vitro*, en células sanas para ver si estos compuestos son selectivos o citotóxicos.
Palabras clave: 2,9-diformil-4,7-difenil-1,10-fenantrolina; reducción; oxidación; compuestos de coordinación con metales esenciales; concentración inhibitoria IC$_{50}$

Introduction

In 1965 Rosenberg showed the pharmacologic effect of *cis*-platin when he was working with the bacteria *Escherichia coli*, and showed that this compound, synthesized i*n situ* had an inhibitory effect on the proliferation of the cells. [1] Years after, Rosenberg proved the *cis*-platin and their derivatives on mice with Sarcoma 180 and Leukemia L-1210 and, observed that the compounds inhibited the proliferation of these type of cells. [2]

According to the World Health Organization (WHO) in 2012, one of the most relevant causes of worldwide death is cancer, taking the live of 8.2 million of people in that year included different types. [3, 4] One of the common treatment for these diseases is *cis*-platin and their derivatives. [5] However, platinum-based compounds have shown to be toxic to the organism, capable to produce damage such as renal dysfunction, allergies, deafness, degenerative changes, etc. [6]

On the other hand, *E. coli* is the most ancient bacteria from which there is record and therefore the most studied microorganism, including the establishment of the mechanisms of DNA duplication. [7] Usually this bacterium lives in human intestine causing chronic diarrhea, infection in the urinary tract, and meningitis and it is mainly spread by poor hygiene on food. [7] Currently, the worldwide population is facing the emergence of new bacterial strains resistant to the known drugs used commonly in the treatment of this disease. [8]

As occurred with bacteria, protozoa also have developed resistance to currently employed treatments, being the amoebiasis a clear example. Amoebiasis is caused by *Entamoeba histolytica,* infecting half million people worldwide and is the second cause of mortality from parasitic disease with 100,000 deaths annually. [9] Its spreading is mostly through fecal-oral route, by ingestion of cysts and also through unclean vegetables fertilized by feces, and foods and water handled by unclean hands. Acute amoebiasis can present symptoms as diarrhea or dysentery with frequent and often bloody stools; whereas chronic amoebiasis can present gastrointestinal symptoms plus fatigue, weight loss and occasional fever. [10] The usual treatments include nitroimidazoles such as metronidazole, ornidazole or tinidazole whose action mechanism involve the generation of reactive oxygen species and direct interaction with DNA. [11]

All mentioned systems (tumoral cells, bacteria and protozoa) have common features: They live and duplicate inside a host organism without killing it in the early stages, they have uncontrolled reproduction and, their most exploitable feature, they are sensitive to induced oxidative stress. [12, 13]

The coordination compounds using essential divalent ions like iron, cobalt, nickel, copper and zinc with the ligand **(L1)** have shown to be effective against the proliferation of different type of human tumor cells like HeLa and CHP-212 and also *Entamoeba histolytica* trophozoites through the induction of a redox unbalance within the treated cells. [12]

For these reasons it has been decided to explore the capacity of the ligand 2,9-biformyl-4,7-diphenyl-1,10-phenanthroline and its corresponding coordination compounds with essential divalent ions to inhibit the proliferation of human neuroblastoma cells CHP-212, *Escherichia coli* and trophozoites of *Entamoeba histolytica* HM1:IMSS cultures. The coordination compounds generated with this ligand and the essential metals have shown from regular to good activities compared with their respective first option drugs.

Experimental

Methods and materials

2,9-dimethyl-4,7-diphenyl-1,10-phenanthroline, $FeCl_2 \cdot 4H_2O$, $CoCl_2 \cdot 6H_2O$, $Ni(NO_3)_2 \cdot 6H_2O$, $CuCl_2 \cdot 2H_2O$, $ZnCl_2$, SeO_2 and tetrabutylammonium hexafluorophosphate were obtained from Sigma Aldrich and used without previous purification. The solvents p-dioxane, DMSO, chloroform, acetone and methanol were obtained from J. T. Baker. DMSO 99.7% Extra Dry over molecular sieve Acros Organics was used for electrochemical experiments and solvents were used without previous treatment.

Synthesis

2,9-diformyl-4,7-diphenil-1,10-phenanthroline (L1). The synthetic pathway was modified from the procedure reported by Chandler. [14] Briefly, 5.5 mmol (2 g) of 2,9-dimethyl-4,7-diphenyl-1,10-phenanthroline was dissolved in p-dioxane (75 mL) under reflux until the complete solubilization of the solid. After 5 min of reflux, 11.0 mmol (1.22 g) of SeO_2 were added to the reaction mixture. Final solution was kept under reflux by two additional hours. After this time, the reaction was filtered over an activated carbon bed. After solvent evaporation, the mixture of solid and hot $CHCl_3$ was filtered a second time. This process was repeated until a white powder was obtained. Total yield after recrystallization was 82%. Elemental Analysis calculated for $C_{26}H_{16}N_2O_2 \cdot 0.5H_2O$ (M. W. = 397 g mol^{-1}) %C: 78.59, %H: 4.03, %N: 7.05. Found: %C: 78.30, %H: 3.72, %N: 7.36. ^1H-NMR (400 MHz, $CDCl_3$) δ = 10.30(s, 1H), 8.32 (s, 1H), 8.08 (s, 1H), 7.56 (m, 5H). ^{13}C-NMR (70 MHz, $CDCl_3$) δ = 193.56, 151.98, 150.58, 146.68, 136.80, 129.60, 129.20, 128.91, 126.66, 120.68. ESI-MS: *m/z* (%): 388 (72) $[M]^+$, 359 (100) $[M-CO-H]^+$, 331 (30) $[M-2CO-H]^+$, 253 (10) $[M-2CO-2H-C_6H_5]$. UV (DMSO): nm (ε, $cm^{-1} M^{-1}$): 290 (20363), 342 (14212)

General synthesis of coordination compounds

L1 was dissolved (194 mg, 0.5 mmol) in a hot mixture of $CHCl_3$-MeOH (50 mL, 3:1 v/v). This solution was added to methanol (50 mL) which contained the corresponding first row salt of the metal, $FeCl_2 \cdot 4H_2O$, $CoCl_2 \cdot 6H_2O$, $Ni(NO_3)_2 \cdot 6H_2O$, $CuCl_2 \cdot 2H_2O$, $ZnCl_2$ (0.5 mmol). The reaction was kept by 30 min under constant stirring. After this time, the solvents were evaporated under atmospheric conditions and the corresponding

powder of the coordination compounds was obtained. The powders were dissolved in CHCl$_3$ adding water and an extraction was performed, collecting the organic phase. After it was collected, the solvent was evaporated under atmospheric conditions.

[Zn(L1)Cl$_2$]. Yellow powder, 79% yield. Elemental Analysis Calculated for [Zn(C$_{26}$H$_{16}$N$_2$O$_2$)Cl$_2$] (M. W = 524.73 g mol^{-1}) %C: 59.51, %H: 3.07, %N: 5.33. Found: %C: 58.63, %H: 2.97, %N: 5.54. UV (DMSO): nm (ε, cm^{-1} M^{-1}): 290 (42926), 342 (23461). Λ (MeOH) = 10.23 S cm^2 mol^{-1}. μ_{eff} = 0.142 MB (0 unpaired electrons). ^{1}H-NMR (400 MHz, CDCl$_3$) δ = 8.14 (d, J = 6 MHz, 1H), 8.05 (s, 1H), 7.58 (m, 5H), 6.33 (d, J = 3.6 MHz, 5H). ^{13}C-NMR (70 MHz, CDCl$_3$) δ = 193.56, 151.98, 150.58, 146.68, 136.80, 129.60, 129.20, 128.91, 126.66, 120.68.

[Cu(L1)Cl$_2$]. Dark-yellow powder, 82% yield. Elemental Analysis Calculated for [Cu(C$_{26}$H$_{16}$N$_2$O$_2$)Cl$_2$]·1.5H$_2$O (M. W.. = 549.88 g mol^{-1}) %C: 56.78, %H: 3.48, %N: 5.09. Found: %C: 57.00, %H: 3.62, %N: 5.34. UV (DMSO): nm (ε, cm^{-1} M^{-1}): 288 (24761), 340 (13128), 468 (6741), 760 (48.21) Λ (MeOH) = 55.30 S cm^2 mol^{-1}. μ_{eff} = 1.502 MB (1 unpaired electron).

[Ni(L1)(NO$_3$)$_2$]. Pale-green powder, 71% yield. Anal. Calc. for [Ni(C$_{26}$H$_{16}$N$_2$O$_2$)(NO$_3$)$_2$]·H$_2$O (P. M. = 589.13 g mol^{-1}) %C: 53.00, %H: 3.07, %N: 9.50. Found: %C: 51.24, %H: 3.06, %N: 9.50. UV (DMSO): nm (ε, cm^{-1} M^{-1}): 290 (33403), 342 (18270), 652 (72.11). Λ (MeOH) = 59.31 S cm^2 mol^{-1}. μ_{eff} = 2.822 MB (2 unpaired electrons).

[Co(L1)Cl$_2$]. Dark-green powder, 86% yield. Anal. Calc. for [Co(C$_{26}$H$_{16}$N$_2$O$_2$)Cl$_2$]·2.5H$_2$O (M. W. = 563.29 g mol^{-1}) %C: 55.43, %H: 3.37, %N: 4.97. Found: %C: 54.21, %H: 3.75, %N: 5.36. UV (DMSO): nm (ε, cm^{-1} M^{-1}): 290 (25207), 342 (13614), 678 (61.27) Λ (MeOH) = 66.65 S cm^2 mol^{-1}. μ_{eff} = 3.907 MB (3 unpaired electrons).

[Fe(L1)Cl$_2$]. Brown powder, 64% yield. Anal. Calc. for [Fe(C$_{26}$H$_{16}$N$_2$O$_2$)Cl$_2$]·4H$_2$O (M. W. = 587.23 g mol^{-1}) %C: 53.17, %H: 4.11, %N: 4.77. Found: %C: 52.75, %H: 3.94, %N: 5.16. UV (DMSO): nm (ε): 286 (30023), 328 (15245), 482 (55.14). Λ (MeOH) = 76.20 S cm^2 mol^{-1}. μ_{eff} = 4.769 MB (4 unpaired electrons).

Single crystal X-ray diffraction

Suitable single crystal for X-ray diffraction experiments was obtained by slow evaporation of CHCl$_3$ of a concentered solution of L1. X-ray diffraction data collection was performed on an Oxford Diffraction Gemini-Atlas diffractometer. [15] The double pass method of scanning was used to exclude any noise. The collected frames were integrated by using an orientation matrix determined from the narrow frame scans. Final cell constants were determined by a global refinement; collected data were corrected for absorbance by using analytical numeric absorption correction using a multifaceted crystal model based on expressions upon the Laue symmetry using equivalent reflections. Structure solution and refinement were carried out with the SHELXS-2014 and SHELXL-2014 packages. [20a] WinGX

v2014.1 software was used to prepare material for publication. .[20b]. Full-matrix least-squares refinement was carried out by minimizing (Fo^2 – Fc^2)^2. All atoms different to hydrogen were refined anisotropically. H atoms attached to C atoms were placed in geometrically idealized positions and refined as riding on their parent atoms, with C–H = 0.95Å and with Uiso(H) = 1.2Ueq(C) for aromatic and methine groups. Crystal data and experimental details of the structure determination of L1 are listed in Table 1.

The crystallographic data for the structure reported in this paper has been deposited with the Cambridge Crystallographic Data Centre as supplementary publication no. CCDC 1520900. Copies of the data can be obtained free of charge on application to CCDC, 12 Union Road, Cambridge, CB2 1EZ, UK (fax: (+44) 1223-336-033, e-mail: deposit@ccdc.cam.ac.uk).

Electrochemical measurements.

All measurements were carried out with a 1 mM concentration of the compounds in anhydrous DMSO and in the presence of 0.1 M tetrabutylammonium hexafluorophosphate as supporting electrolyte, using a potentiostat/galvanostat BioLogic SP-50. A

Table 1. Crystallographic data for L1

Empiric formula	C$_{28}$ H$_{18}$ Cl$_6$ N$_2$ O$_2$
Molecular weight	627.14
Temperature (K)	130(2)
Wave length (Å)	0.71073
Crystal system	Monoclinic
Space group	P 21/c
A (Å)	15.2053(3)
B (Å)	15.7277(2)
C (Å)	12.3190(2)
Volume (Å^3)	2799.66(9)
Z	4
Density (calc) mg m^{-3}	1.488
Abs coef., μ mm^{-1}	0.644
F(000)	1272
Theta range data collection	3.324 a 28.271°
Collected difractions	59124
Independent reflections	6642
Completeness to theta	99.80%
Refinement method	Full-matrix least-squares on F^2
GOF on F^2	1.045
Final R indexes	R$_1$=0.0375
[I>2σ(I)]	wR$_2$=0.0907
R indexes all data	R$_1$=0.0474 wR$_2$=0.0973
Largest diff. Peak and hole (e Å^3)	0.063, -0.673

typical three electrodes arrangement was employed with a carbon vitreous disk as working electrode. A platinum wire was used as a counter electrode, and a silver wire as a pseudo-reference electrode. Before the voltammetric experiments, the solution was bubbled during 5 min with nitrogen. All cyclic voltammograms were started from open potential circuit (E_{opc}), at scan rate of 0.1 V s^{-1} in a negative direction. Ferrocene was added as internal reference at the end of the measurements. Redox potentials are reported against the pair Fc^+/Fc according the IUPAC recommendations. [17] Ohmic drop compensation was corrected using positive feed-back.

Biological assays

Human tumor cell line CHP-212

In vitro antiproliferative activity was evaluated according to the procedure described by Skehan. [18] Briefly: 2 x 10^4 CHP-212 cells (Human neuroblastoma) were seeded in 96-well plates and they were incubated during 24 h at 37°C and 5% of CO_2. After incubation time the DMEM F-12 medium was changed and new medium was added with 10 µL of the compounds at final concentrations 1, 3, 10 and 30 µg/mL. The cells were exposed to the compounds during 24 h with the same incubation conditions described above, after that, the medium was removed once again and the cells were fixed into the plate with trichloroacetic acid (TCA) 10% during 1 h at 4°C. The fixed cells were stained with 50 µL of sulforhodamine B 0.4 % during 30 min and washed with acetic acid 1% to remove the excess of colorant. Once the plates were dried the colorant was redissolved with Trizma buffer (pH = 10). The absorbance of the plates was measured with a microplate reader at 540 nm. From the absorbance of the plates, the inhibitory percentage was calculated according the equation: % inhibition = 100-(100 X [T/C]) where T is the absorbance of the treated cells and C is the absorbance of the cells treated with vehicle DMSO 0.1 %v/v. The IC_{50} was determinate from the construction of a dose-response curve where the corresponding value is interpolated. This dose-response curve was the half of three independent assays of the evaluated compounds.

Escherichia coli BL 21

Cell solutions. A single colony of *Escherichia coli* BL21(DE3) was inoculated in Luria-Bertani (LB) liquid media and incubated overnight at 37°C. Then, 1.5 mL of cell culture was centrifuged and the medium replaced with 0.85% NaCl solution. The optical density at 670 nm (OD_{670nm}) was adjusted to 0.02 with 0.85% NaCl solution and dilutions of 1:10 000 and 1:100 000 were made.

Medium. Sterile molten (44°C) LB agar was supplemented with either ampicillin (as a positive control of antibiotic), and DMSO, ligand (L1) or one of the coordination compounds (Fe(L1)Cl$_2$, Co(L1)Cl$_2$, Ni(L1)(NO$_3$)$_2$, Cu(L1)Cl$_2$, Zn(L1)Cl$_2$).

The aqueous ampicillin solution and H$_2$O-DMSO (99%:1% v/v) coordination compounds solutions were prepared and filtered with a 0.2 µm pore size filter. The final concentrations of ampicillin in the broth were: 2.86 µM, 28.6 µM and 286 µM; DMSO was added at 1% v/v, and the ligand and coordination complexes concentrations were: 8.8 µM, 17.6 µM and 35.2 µM.

Pour plate method and plate count. 100 µL of cell solution were pipetted into a sterile plate. Sterile molten LB agar was added and mixed completely with the inoculum. The culture was then incubated overnight at 37°C. The CFU on and under the solidified medium were counted. This was done for duplicate for each one of the dilutions.

## Parasite culture and amoebicidal activity

Entamoeba histolytica HM1: IMSS trophozoites were axenically grown in TYI-S33 medium.[24] Trophozoites (1 × 10^5) were placed in tubes with 3 ml of TYI-S33 medium and each compound was added to reach the final concentrations as follows: 1000, 100, 10, 1, 0.1 and 0.01 µM. Amoebic trophozoites viability was assessed employing optical microscope with vital marker trypan blue and confirmed through the fluorescent dyes carboxyfluorescein diacetate (CFDA) and propidium iodide. Trophozoite viability determinations were done at 24, 48 and 72 h. Briefly, samples of 100 µl containing 1×10^4 treated parasites were added with 100 µl trypan blue 0.4% and cell viability were determined with a haemocytometer in an optical microscope. An independent trophozoites culture sample (≈1 × 10^4) was received 1 µl of 5 µM CFDA (Invitrogen, USA) containing 1 µl of 1.5 µM propidium iodide. The final solution was mixed and incubated at room temperature for 15 min. Viable cells were counted using the fluorescent microscope Olympus BX51.

Results and discussion

Synthesis and characterization

In order to synthesize the compound 2,9-diformyl-4,7-diphenyl-1,10-phenanthroline (L1) a modification of the synthetic route reported by Chandler was used, the modification involves the stoichiometry of SeO$_2$ (two equivalents instead of five) and reaction time (the reaction was kept under reflux for two hours). (Scheme 1).

Once L1 was obtained and purified, it was dissolved (0.5 mmol, 194 mg) in a hot mixture of CHCl$_3$-MeOH (3:1, % v/v) and it was added to a solution of methanol (15 mL) which contained the corresponding first row metal salt FeCl$_2$·4H$_2$O, CoCl$_2$·6H$_2$O, Ni(NO$_3$)$_2$·6H$_2$O, CuCl$_2$·2H$_2$O or ZnCl$_2$ (0.5 mmol). After the addition was completed, the reaction was left 30 min in constant stirring. After this time, solvents were evaporated under atmospheric condition, until the corresponding powders of the coordination compounds was obtained (Scheme 2).
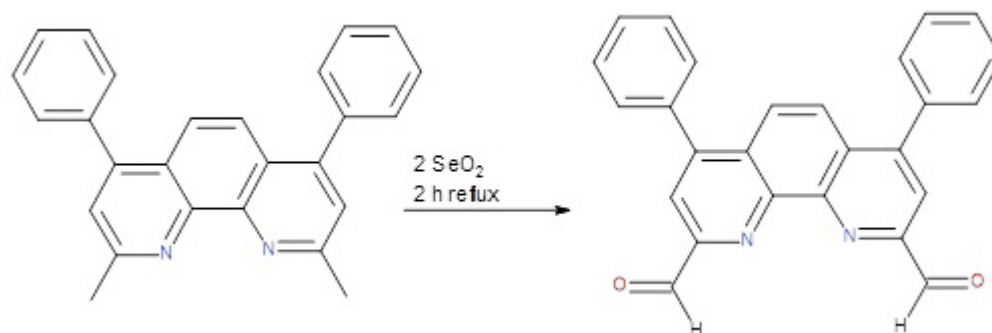
Scheme 1: synthetic pathway for the preparation of 2,9-diformyl-4,7-diphenyl-1,10-phenanthroline (L1).
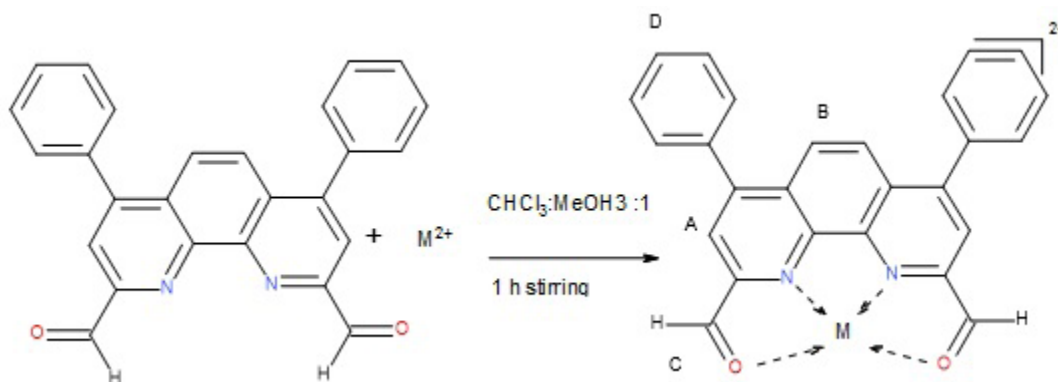
Scheme 2. Synthetic pathway for the synthesis of [ML1]

The ^{1}H-NMR was obtained for L1 and the coordination compound [ZnL1Cl$_2$]. These spectra were acquired to determine the coordination sphere of the metal ion. The chemical shifts found for L1 and [ZnL1Cl$_2$] are shown in Table 2.

L1 presents four signals numbered using the code shown in Scheme 2. The protons A, B and D of ZnL1do not appear to have a significant displacement compared with L1. However, proton C is not only changing its shift, but also the multiplicity. The other proton in which the multiplicity has been modified is the proton A. Protons A and C, in L1 are singlets, but in the presence of the metal, the multiplicity changes to a doublet. In the COSY experiment exists a coupling of the proton A and C, which indicates that these protons are close enough to produce the splitting of the signals. In the ^{1}H-NMR spectrum of L1 this coupling does not exist, because the constant rotation of the aldehyde C-H bond so this is why these protons are singlets; meanwhile, the coordination of the oxygen atoms from the

aldehyde to the metal ion avoids this rotation fixing the position of the aldehyde's hydrogen that is now capable to couple with proton A.

Structural characterization

The ORTEP plot of L1 is shown in Fig. 1, includes two molecules of chloroform were found in the unit cell as solvation. Selected bond lengths and angles are given in Table 2. The corresponding structure and atom labeling are shown in Fig. 1.

The three aromatic rings of phenantroline system are coplanars with rms deviation of fitted atoms of 0.022, then this plane shows the angles of 52 and 61°with the phenyl rings formed by C15-C16-C17-C18-C19-C20 and C21-C22-C23-C24-C25-C26 respectively. In the crystalline array there are C-H···N and C-H···Cl intermolecular interactions of type hydrogen bond. The two interactions C27-H27···N1 (2.41 Å) and C27-H27···N2 (2.45 Å) forming the *(5) motif.*

Electrochemical studies

Fig. 2 shown the cyclic voltammogram of L1, acquired from open circuit potential to negative direction ($E_{\lambda-}$), where three reduction signals (I_c, II_c, III_c), and three oxidation signals (I_a,

Table 2. Chemical shifts (ppm), multiplicities of ^{1}H-NMR spectra of L1 and [Zn(L1)Cl$_2$]

Proton	L1	[Zn(L1)Cl$_2$]
A	8.31 (s)	8.14 (d, 6 MHz)
B	8.08 (s)	8.05 (s)
C	10.61 (s)	6.33 (d, 3.6 MHz)
D	7.56 (m)	7.58 (m)
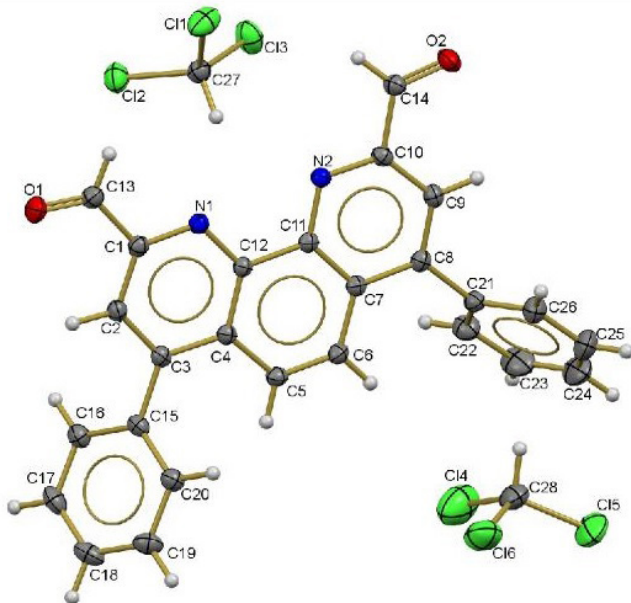
Fig. 1. ORTEP plot (50% probability level) of L1.

Table 2. Selected bond lengths [Å] and angles [°] for **L1**.

|	
Cl(1)-C(27)	1.7664(18)
Cl(4)-C(28)	1.748(3)
O(2)-C(14)	1.208(2)
O(1)-C(13)	1.209(2)
N(1)-C(1)	1.330(2)
N(1)-C(12)	1.352(2)
N(2)-C(10)	1.328(2)
N(2)-C(11)	1.354(2)
C(3)-C(15)	1.486(2)
C(10)-C(14)	1.489(2)
C(12)-C(11)	1.455(2)
C(8)-C(21)	1.489(2)
C(1)-C(13)	1.488(2)
C(1)-N(1)-C(12)	116.90(13)
C(10)-N(2)-C(11)	116.83(14)
O(1)-C(13)-C(1)	123.36(16)
O(2)-C(14)-C(10)	123.00(16)
Cl(2)-C(27)-Cl(1)	109.76(10)
Cl(4)-C(28)-Cl(5)	110.45(13)

II_a, III_a) could be observed. Potential inversion studies were performed in order to associate signals dependence. For process I the cathodic potential peak was $E_{pc}(I_c)$ = -1.60 V vs Fc^+/Fc and its corresponding oxidation peak potential was E_{pa} (I_a)= -1.53 vs Fc^+/Fc. For processes II and III, the values found for E_{pc} were -1.83 vs Fc^+/Fc and -2.01 V vs Fc^+/Fc respectively,

while the values of E_{pa} were -1.50 V vs Fc^+/Fc and -1.94 V vs Fc^+/Fc respectively. For all the process, the differences between anodic and cathodic peak potential values and the linear relationship I vs $v^{1/2}$, suggest reversible electron transfers controlled by diffusion. The half-wave potentials ($E_{1/2}$) were calculated and corresponded to, I = -1.57 V vs Fc^+/Fc, II =-1.79 V vs Fc^+/Fc and III = -1.97 V vs Fc^+/Fc, respectively. Process I is related to generation of a radical anion L+1e→L$^{•-}$. The second electron transfer for process II generates a radical di-anion species, L$^{•-}$+1e→L$^{•2-}$. According to literature, both redox processes are centered at carbonyl moieties. [19] The low current values for signals in processes III_c and III_a, in comparison with those observed at I and II, could be attributed to a self-protonation reduction process of the radical di-anion species. The comproportionation constant (K_{com}) from the processes I and II, was evaluated according with the literature for an EE [21] mechanisms. L1 shows a K_{com} = $10^{4.22}$ suggesting that this system belongs to the second class compound, according to the Roby-Day classification. This implies that there exists a slightly delocalization of the charge and a slightly electronic communication between both redox centers, consistent with the results found. [21]

To demonstrate the proposed mechanism, a donor proton was added to the system. Fig. 3 shows the cyclic voltammograms of L1 in the absence and in the presence of 1 mmol of acetic acid (HA). In the presence of HA, a shift to positive values for potential peaks with an increase in current for the reduction process I_c and II_c (I'_c and II'_c) are observed. Additionally, the process III and the corresponding oxidation signals for I_c and II_c are not recorded. This behavior is typical for a proton-coupled electron transfer (PCET), which involves a bi-electronic reduction for each process that could probably generate alcohol species from the aldehydes moieties within the ligand L1. The third reduction is no longer appreciable due to the instability a di-anion species in a protic medium. This evidence
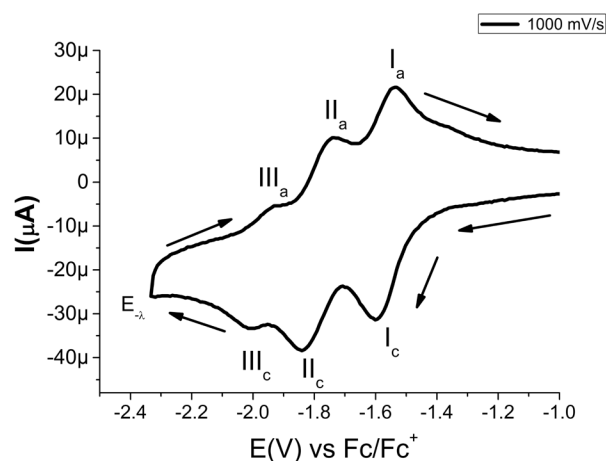
Fig. 2. Cyclic voltammogram for 1 mM of L1 in DMSO + 0.1 M TBAPF$_6$. The scan potential was initiated from E_{opc} to negative direction. The working electrode was vitreous carbon. Scan rate 1 V/s.
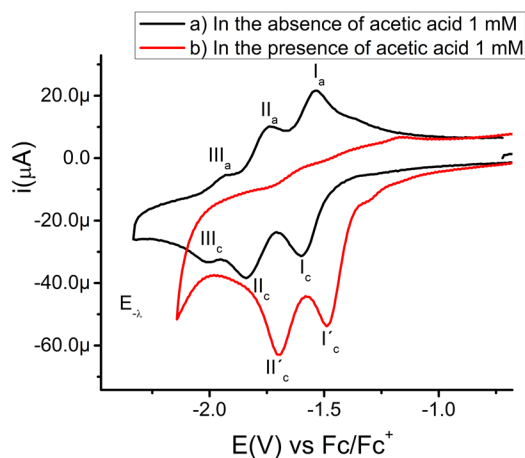
Fig. 3. Cyclic voltammogram for 1 mM of L1 in DMSO + 0.1 M TBAPF₆ (a) in the absence and (b) in the presence of 1 mM of Acetic Acid. The scan potential was initiated from E₀ₚ𝒸 to negative direction. The working electrode was vitreous carbon.

confirms that redox processes takes place at carbonyl groups of aldehydes.

Fig. 4a presented a typical voltammogram of [CuL1], where one reduction process (IV_c) and one oxidation process (IV_a) can be observed. The relationship between the signals is confirmed in a switching potential experiment at $E_{-\lambda}$= -1.0 V vs Fc-Fc⁺. The process (IV) corresponds to the electrochemical reaction [Cu^{II} (L1)]→[Cu^{I} (L1)]. The half-wave potential value for the redox couple [Cu(L1)]²⁺/[Cu(L1)]⁺ is -0.198 V *vs* Fc⁺/Fc, with a quasi-reversible behavior, ΔEp=0.501 V, due to the high reorganization energy of copper species in DMSO. On the other hand, in an experiment using a more negative switching potential at $E_{-\lambda}$= -2.0 V vs Fc-Fc⁺, the redox process associated the ligand (I, II, and III), are observed at less negative values in comparison with the free ligand L1. The change in the oxidation state of the metal center accompanied and the modification of the geometry in the reduction process I_c, affect the electronic distribution within all the compound, causing a decrease in the energy requirements of processes I and II.

The coordination compounds of cobalt(II), iron(II), nickel(II) and zinc(II), lack of the metal-associated redox processes but the ligand-associated signals appear displaced to less negative potential values (see Figures. 5a and 5b). The oxidation processes I_a do not have the same current intensity as its corresponding reduction processes I_c, which may be attributed to the reduction of aldehyde moiety to a non-electroactive moiety, probably to alcohol catalyzed by the metal center in the reduced species M-L•⁻. This behavior is similar to that recorded for the reduction of non-coordinated ligand L1 in the presence of HA. Due the electroactive window it was not possible to see the oxidation process associated with the metal, probably because these values are higher than the anodic barrier. Additionally, low current values for processes II_c and III_c, for electro-generated species or self-protonation processes are recorded for all compounds. However, only the main process I_c, is considered

to understand biological activities. A summary is presented in Table 3.

The reduction potential peak values associated to L1 for the free ligand and in the coordination compounds are shown in table 3.

As it is shown Table 3, the reduction potentials of the ligand in the coordination compounds, are less negative than L1, so less energy is required to achieve the reductions of the carbonyls in the coordination compounds.

Biological assays

Assays in CHP-212 cells

The CHP-212 cells were seeded during 24 h at 37 °C and 5% of CO₂. All the compounds were evaluated using a solvent mixture of H₂O-DMSO (9:1 %v/v). The results are reported as

**Table 3.** Reduction potentials of the ligand in the coordination compounds.

Compound	$E_{pc}(I_c)^a$	$E_{pc}(II_c)^a$	$E_{pv}(III_c)^a$
[Fe(L1)Cl₂]	-1.51	-1.72	---
[Co(L1)Cl₂]	-1.54	-1.79	-1.97
[Ni(L1)(NO₃)₂]	-1.58	-1.82	-1.99
[Cu(L1)Cl₂]	-1.32	-1.51	-1.69
[Zn(L1)Cl₂]	-1.58	-1.83	---
L1	-1.60	-1.85	-2.01

a = V Vs Fc-Fc⁺, obtained in DMSO in presence of 0.1 M TBAPF₆. The working electrode was vitreous carbon. Scan rate 1 V s⁻¹
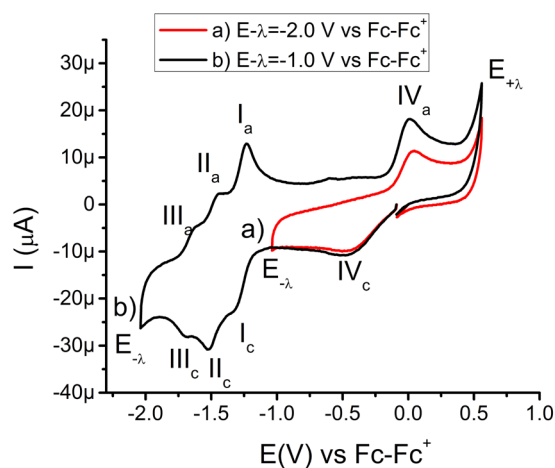
Fig. 4. Cyclic voltammogram for 1 mM of [Cu(L1)Cl₂] in presence of 0.1 M TBAPF₆. The scan potential was initiated from E₀ₚ𝒸 to negative direction, switching the potential at (a)- 1.0 V *vs* Fc-Fc+ and (b)- 2.0 V *vs* Fc-Fc+. The working electrode was vitreous carbon. Scan rate 1 V s⁻¹.
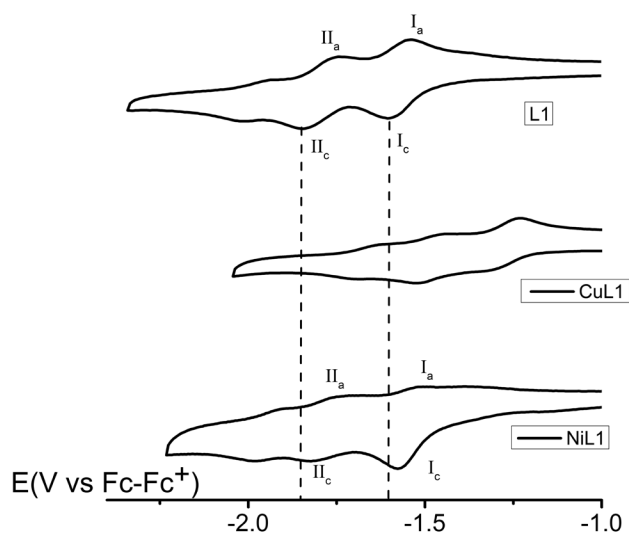
Fig. 5a. Cyclic voltammograms for 1 mM of L1, and [M(L1)] M= Cu, and Ni in DMSO in presence of 0.1 M TBAPF$_6$. The scan potential was initiated from E$_{opc}$ to negative direction. The working electrode was vitreous carbon. Scan rate 1 V s^{-1}
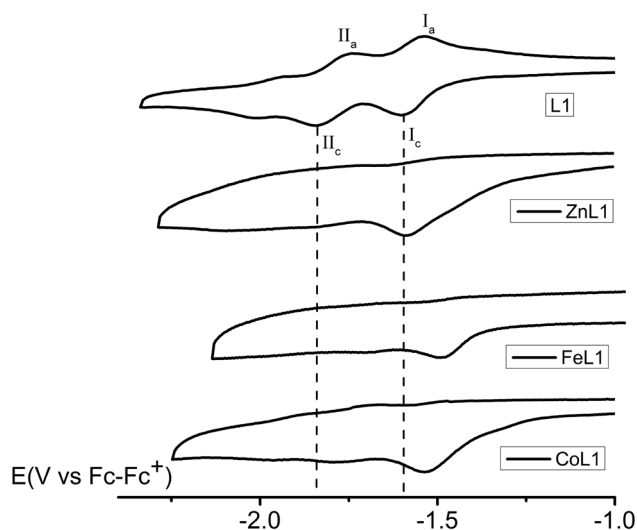

Fig. 5b. Cyclic voltammogram for 1 mM of [M(L1) M= Zn, Fe, Co in presence of 0.1 M TBAPF$_6$. The scan potential was initiated from E$_{opc}$ to negative direction. The working electrode was vitreous carbon. Scan rate 1 V s^{-1}

IC$_{50}$, which is the necessary concentration to inhibit the 50% of the cellular proliferation (Table 4). The assays were performed at a final concentration of 0.1 % v/v of DMSO, which presented a 1% of inhibition. The IC$_{50}$ value of *cis*-platin is presented as comparison due to is a compound already used in treatment.

All coordination compounds present a higher capacity to inhibit the proliferation of human neuroblastoma cell cultures than *cis*-platin which is the commonly drug used in the treatment of cancer. The most active compound, the iron (II)

compound with an IC$_{50}$ = 31.99 μM, is 7 times more potent than the *cis*-platin (IC$_{50}$ = 226.70 μM) as cell growth inhibitor. This biological activity could be correlated with the first electron gain of the ligand, which it is also the most oxidant of the compounds evaluated. On the other hand, compound [CuL1Cl$_2$] showed the higher IC$_{50}$ of 141.25 μM but still is 1.6 fold more active than *cis*-platin. For this compound having the lowest reduction potential for the process associated to the ligand within the coordination compounds, the metal center also presents a redox activity, so the mechanistic pathway to induce cellular damage must be different than the other compounds studied in this work, which is clearly observed in fig. 6. In our research group has been studied the action mechanism of Cu(II) coordination compounds , the results have shown that are capable to inhibit the proliferation by the generation of reactive oxygen species (ROS) and thorough the direct interaction with DNA. [22, 23]

The results of the coordination compound of copper inhibiting the proliferation of CHP-212 cultures are in agreement with other compounds synthesized by our research group, that is Casiopeínas®,[22, 23] and CuN6 (N6= 2,9-bis-(2',5'-diazahexanyl)-1,10-phenanthroline [12] where the redox potential of the metal center plays an important role in its anti-proliferative activity. Following this tendency, all the coordination compounds within the redox potential range -0.5 to 0.5 V vs Fc$^+$|Fc can be good candidates to keep searching for possible drugs to combat cancer. A possible mechanism of action of the coordination compounds of iron, cobalt, nickel, zinc, and with L1, remains to be elucidated but comparing with compounds reported, [9] we propose that a redox unbalance must be involved provoked by the redox activity of L1.

Assays in *Escherichia coli*

Results are expressed as IC$_{50}$ and are shown in Table 5. All the coordination compounds showed slightly antibacterial activity, except [FeL1Cl$_2$]. Their IC$_{50}$ values showed in all cases an effect comparable with that observed for ampicillin. The control experiment with 1% DMSO did not show antimicrobial activity.

The coordination compound with the lowest IC$_{50}$ is [Zn(L1)Cl$_2$] with a value of 5.52 μM, in contrast with the results obtained for CHP-212 cells, which was [Fe(L1)Cl$_2$]. In the case of the assays in *E. coli* the coordination compound with

Table 4. IC$_{50}$ of the tested compounds in CHP-212 cells

Compound	IC$_{50}$ (μM)
[Fe(L1)Cl$_2$]	31.99
[Co(L1)Cl$_2$]	42.98
[Ni(L1)(NO$_3$)$_2$]	109.65
[Cu(L1)Cl$_2$]	141.15
[Zn(L1)Cl$_2$]	133.27
L1	201.27
Cis-platin [12]	226.70
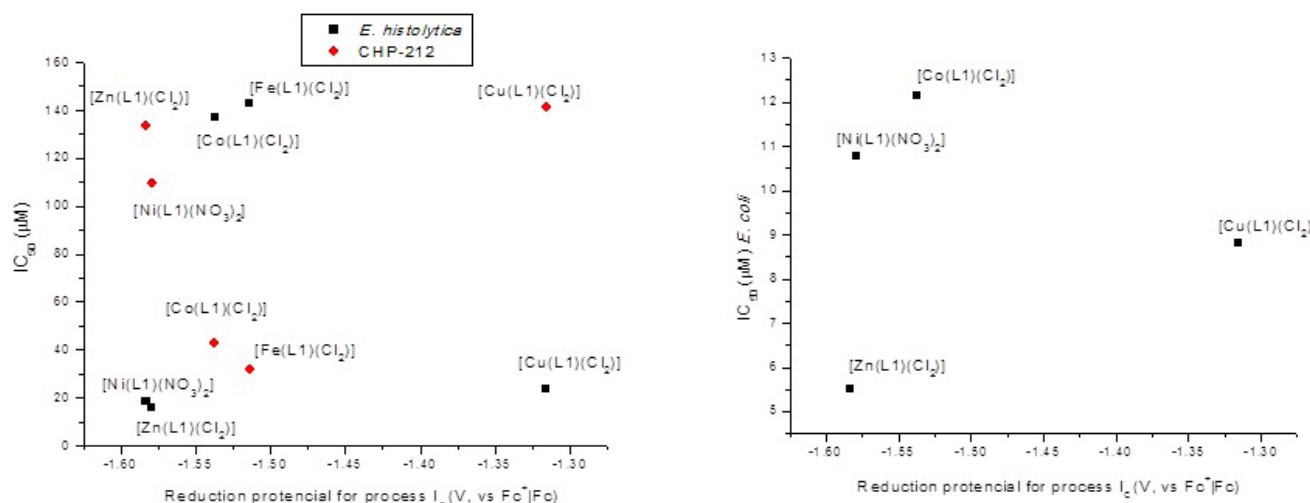
Fig. 6. Correlation between the reduction potential for process Ic and the IC_{50} against three different type systems, CHP-212 cells, *E. coli* and *E. histolytica* respectively.

Table 5. IC_{50} of tested compounds in *E. coli*.

Compound	IC_{50} (µM)
[Fe(L1)Cl$_2$]	NA*
[Co(L1)Cl$_2$]	12.16
[Ni(L1)(NO$_3$)$_2$]	10.78
[Cu(L1)Cl$_2$]	8.80
[Zn(L1)Cl$_2$]	5.52
L1	19.95
Ampicillin	1.23

*NA: showed no antimicrobial activity.

the more negative redox potential was the most active (the less oxidant). When compared with the ligand alone, the presence of the metal center increased the activity of the molecule.

The copper compound as it was observed in the assays in CHP-212 cells, leaves the tendency. This is explained because it has a reduction redox potential associated with the metal, and the mechanistic via must be different than the other coordination compounds tested.

Assay in Entamoeba histolytica

Finally, the amoebicidal activity of the synthesized compounds was also evaluated. As observed with the bacteria cultures, none of the compounds showed better activity than the first election drug, however, it is interesting to remark the similarity of the biological activity against both, bacteria and parasites, when is analyzed as a function of the redox potential of the compounds.

The better amoebicidal activity was presented by [Ni(L1)(NO$_3$)$_2$] with IC_{50}= 16 µM, followed by [Zn(L1)Cl$_2$] with IC_{50}=

18.3 µM. In a general way, as the redox potential becomes more positive, the amoebicidal activity decreases, with exception of compound [CuL1Cl$_2$]. This compound has to exert a different mechanism due to is the only one in which the metal ion can be reduced.

From Fig. 6 it is clear that with exception of the Cu(II) compound, as the redox potential becomes more negative the antiproliferative activity over human tumor cells decreases. On the other hand, just the opposite behavior is observed when the compounds were administered to bacteria and trophozoites cultures.

The behavior found with the compounds studied in this work in trophozoite cultures is similar to that stated before with MN6 compounds [12]. The effect of metal coordination sphere modification is evident in the IC_{50} values obtained for both families, being at least one order of magnitude most potent the compounds with the ligand N6(see table 6). This could be due to the stability of the compound compared with those obtained with the ligand 2,9-diphormyl-4,7-diphenyl-1,10-phenanthroline.

It is important to remark the similarity in the antiproliferative activity of the evaluated coordination compounds in bacteria and trophozoites. Even though any of them possess a better antiproliferative activity than the first election drugs, all the

Table 6. IC_{50} of tested compounds in *E. histolytica*

Compound	IC_{50} (µM)	MN6 (µM)
[Fe(L1)Cl$_2$]	142.6	NA
[Co(L1)Cl$_2$]	137.26	0.8
[Ni(L1)(NO$_3$)$_2$]	16.0	0.06
[Cu(L1)Cl$_2$]	23.41	6.0
[Zn(L1)Cl$_2$]	18.32	1.0
Metronidazole	6.7	6.8

compounds that present antibacterial activity exert their action with lower concentrations than that used to inhibit the proliferation of trophozoites. Ampicillin acts as an irreversible inhibitor of transpeptidase, a fundamental enzyme needed by the bacteria to make the cell wall. (Petri WA in Brunton LL, Chabner BA, Knollmann BC (eds.) (2011) Goodman and Gilman's The Pharmacological Basis of Therapeutics, 12th ed., Chapter 53. McGraw-Hill, New York). On the other hand, the mechanism of action of metronidazole is principally associated to the direct interaction with DNA and ROS production. However, the use of this compound in therapy is not limited to the protozoa, being also active in gram-positive and gram-negative bacteria. [25] (The effectiveness of metronidazole in bacteria and protozoa is related with the presence of the enzyme pyruvate:ferredoxine oxidoreductase (POR). This enzyme is shared by luminal protozoa and bacteria and is the responsible to reduce the ferredoxin or flavodoxin which in turn transfers an electron to metronidazole to activate it. [26] The fact that coordination compounds evaluated in this work present a great similarity in their antiproliferative activity in both, bacteria and protozoa, strongly suggest that an additional molecular target must be explored, the interaction with POR. It is then very important to highlight the fundamental role played by the compounds' redox potential to produce the antiproliferative activity and promote the exploration of new compounds guided by this parameter that could be active in all three systems, tumor cells, protozoa and bacteria.
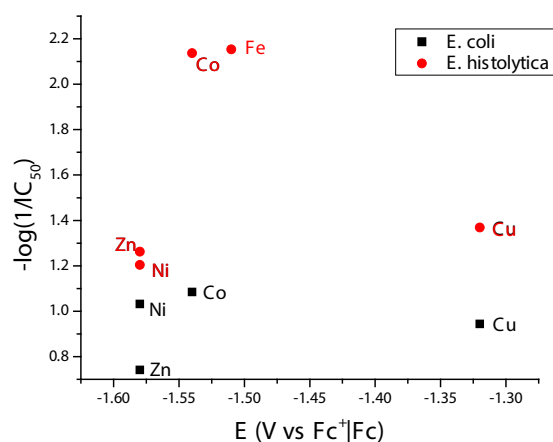
Conclusions

The ligand L1 and its coordination compounds with different first-row metals were synthesized and fully characterized. The *in vitro* antiproliferative preliminary studies of the compounds in CHP-212 cells shown that all the coordination compounds presented a higher activity than *cis*-platin, which is the commonly drug used in the treatment of this cancer. This activity could be correlated with the first potential redox of the ligand in the coordination compounds, being the compound with the

lowest potential value (the more oxidant) the most active against CHP-212 cells. These studies may open a new investigation line employing ligands with two carbonyls capable to generate a bi-radical bi-anion accompanied with transition metals of the first row. Additionally, these compounds presented an anti-bacterial and amoebicidal activity that could be correlated with the same redox process, but with inverse behavior: the compound with the lower negative potential (the less oxidant) was the one who presented the higher activity. It is important to demonstrate that in the systems where the ligand was evaluated, it did not show a higher activity that the observed for the coordination compounds, indicating the metals activate the organic molecule. Also, the cellular systems employed are susceptible to the oxidant stress, which can be induced by the redox activity of the coordination compounds. Furthermore, the great similarity observed in the antiproliferative capacity of these compounds in bacterial and protozoa suggest that the biological activity could involve the interaction of them with the enzyme pyruvate:ferredoxine oxidoreductase (POR), providing very important tools in the development of new wide spectrum drugs. Because these compounds are new, it is important to keep investigating how inhibition occurs, as well as the effect in healthy cells in order to stablish the mechanism of selectivity or cytotoxicity, in the interest of their use as anticancer, antibacterial or amoebicidal drugs.

Acknowledgements

References

1. Rosenberg, B.; Van Camp, L.; Krigas, T.; *Nature* **1965**, 205, 698-699.
2. Rosenberg, B.; Van Camp, L.; Trosko, J. E.; Mansour V. H.; *Nature*, **1969**, 22, 385-386.
3. http://www.who.int/mediacentre/factsheets/fs297/es/accessed   in September, 2016.
4. http://www.who.int/cancer/media/AccionMundialCancerfull.pdf accessed in September, 2016.
5. Moosa, A. R.; Schimpff, S. C.; Robson, M. C.; Williams & Wilkins. Baltimore ed. Vol 1. **1991.**
6. Kui, W.; Jingfen, L.; Ronchang, L.; *Coord. Chem. Rev.*, **1996**, 151, 53-58.
7. Lenhinger, N. D. L.; Freeman, W. H.; Principles of Biochemistry. 4th Ed. **2004.**
8. May, M.; *Nature*, **2014**, 509, 84-85.
9. Health Systems Financing: The Path of Universal Coverage. *The World Health Report 2010*; World Health Organization: Geneva, Switzerland 2010.
10. Fotedar, R.; Stark, D.; Beebe, N.; Marriot, D.; Ellis J.; Harkness, J.Laboratory Diagnostic Techniques for Entamoeba Species. *Clin. Microbiol. Rev.* **2007**, 20, 511-532.

11. Land, K. M.; Johnson, P. J. *Drug Resist. Updates* **1999**, 2, 289-294.

12. García-Ramos, J. C.; Toledano-Magaña, Y.; Talavera-Contreras, L. G.; Flóres-Álamo, M.; Ramírez-Delgado, V.; Morales-León, E.; Ortiz-Frade, L.; Grizett-Guitérrez, A.; Vázquez-Aguirre, A.; Mejía C.; Laclette, J. P.; Moreno-Esparza, R.; Ruiz-Azuara, L.; *Dalton Trans.* **2012**, 41, 10164-10174.

13. Bravo-Gómez, M. E.; Ruiz-Azuara, L.; *Curr. Med. Chem*., **2010**, 17, 3606.

14. Chandler, C. J.; Deady, L. W.; Reiss, J. A.; *J. Heterocycl. Chem*. **1981**, 18, 599.

15. CrysAlis PRO, *and CrysAlis RED*, Agilent Technologies, Yarnton England, **2009.**

16. Sheldrick G. M. *Acta Crystallogr., Sect, A*, **2008**, 64, 112.

17. Gritzner, G.; Küta, J.; *Pure Appl. Chem.*, **1984**, 4, 461.

18. Skehan, P.; Storeng, R.; Scudiero, D.; Monks, A.; McMahon, J.; Vistica, D.; Warren, J. T.; Bokesch, H.; Kenney, S.; Boyd, M. R.; *J. Natl. Cancer Inst.* **1990** vol. 82, no. 13, 1107-1112.

19. Neal, R. A.; Rod, K. Q.; *Analytical Chem.* **1974**, 46 (12), 1759-1764.

20. a) Sheldrick, C.M. Crystal Structure Refinement with SHELXL. Acta Cryst., Sect. C: Found. Crystallogr. 2015, 71, 3-8.; b) Farrugia, L. WinGX Suite for Small-molecule Single-crystal Crystallography J. Appl. Crystallogr. 1999, 32, 837-838.

21. Zanello, P.; Inorganic Electrochemistry, theory, Practice and Application. The Royal Society of Chemistry, Cambridge, UK, **2003.**

22. Bravo-Gómez, M. E.; García-Ramos, J. C.; Gracia-Mora, I.; Ruiz-Azuara, L.; *J. Inorg. Biochem.*, **2009**, 103, 209.

23. a) Trejo-Solis, C.; Palencia, G.; Zuniga, S. A. Rodriguez-Ropon, S.; Osorio-Rico, L.; Luvia, S. T.; Gracia-Mora, I.; Marquez-Rosado, L.; Sanchez, A.; Moreno-Garcia, M. E.; Cruz, A.; Bravo-Gomez, M. E.; Ruiz-Ramirez, L.; Rodriguez-Enriquez, S.; Sotelo, J.; *Neoplasia*, **2005**, 7, 563.
b) Anllely Grizett Gutiérrez, Adriana Vázquez-Aguirre, Juan Carlos García-Ramos, Marcos Flores-Alamo, Enrique Hernández-Lemus, Lena Ruiz-Azuara, Carmen Mejía. *Journal of Inorganic Biochemistry* **2013,** 126, 17-25.

24. L. Diamond. Science. 134 (1962) 336-337.

25. I. Brook, J. Infect. Chemother. 2016, 22, 1-13.

26. Samuelson, J. Why Metronidazole is Active Against Both Bacteria and Parasites. Antimicrob. Agents Chemotherapy. 1999, 43, 1533-1541).